

CONDUCTIVITY DISCONTINUITIES IN THE UPPER MANTLE  
BENEATH A STABLE CRATON

A. Schultz<sup>1</sup>, R.D. Kurtz<sup>2</sup>, A. D. Chave<sup>3</sup>, A. G. Jones<sup>2</sup>

**Abstract.** We present evidence for approximate collocation of seismic and electrical transitions in the upper mantle. More than two years of very long period magnetotelluric (MT) data were recorded at a lakebottom observatory in the central Canadian Shield. After processing to contend with non-stationary source effects, and removal of galvanic distortion, the underlying structure is 1D for periods of one hour to four days. The response was extended to periods of 100 days by appending Geomagnetic Depth Sounding data to the MT curves. Minimum structure linearised inversion, nonlinear extremal inversion, and a new genetic algorithm for nonlinear hypothesis testing, reveal discrete jumps in conductivity at depths near the major upper mantle seismic discontinuities. The jumps occur over limited depth ranges.

INTRODUCTION

Seismic observations have provided the primary constraints for models of mantle structure from the Moho to the base of the mid-mantle transition zone. The possibility of obtaining a wholly independent view of mantle conditions with sensitivity to electrical rather than elastic properties is an exciting prospect, although corresponding progress in electromagnetic imaging of Earth's deep interior has been only modest.

Upper mantle electrical conductivity determined from field measurements ranges between  $10^{-3}$  S/m (or lower) at shallow depths and increases to nearly  $10^1$  S/m at the base of the mid-mantle. Smooth, monotonic conductivity increases are consistent with previous data, as are models containing abrupt jumps in upper to mid-mantle conductivity. The resolving power of such data is too limited to demonstrate conclusively that jumps are strictly required.

The work reported here is the first attempt to examine detailed upper mantle electrical structure beneath a stable craton, the central Canadian Shield. The continental lithosphere may be more homogeneous beneath cratons than below tectonically active areas, increasing the likelihood that mantle conductivity may be regionally 1D. This makes it possible to extract regional conductivity information from a single site for depths spanning the lithosphere-asthenosphere boundary, the proposed Lehmann discontinuity (~205-230 km), and the 410 km and 660 km seismic transitions.

The catalogue of existing very long period MT data is sparse, as there had been technical limitations to earlier equipment, and no obvious solution to the problem of long period electrode drift, which limits the response of conventional MT experiments to periods less than ~10,000s. Conductivity information of somewhat lower resolution may also be extracted from magnetic observatory data through Geomagnetic Depth Sounding (GDS) in the period range of approximately 4 days to 2 years [Schultz & Larsen, 1987]. The gap in coverage between conventional MT and GDS methods, spanning periods of several hours to about a week, corresponds to frequencies associated with greatest resolving power throughout the upper 300-600 km of the mantle.

Lakebottom deployment of longline electric dipole receivers is

one means of ensuring stable long period electric field measurements, with little contamination from drift due to chemical and thermal gradients, and reduced possibility of disruption by cultural noise and physical damage [Schultz et al, 1987]. We have built on this idea to extend the response bandwidth into the long period gap between conventional MT and GDS responses, leading to greatly enhanced resolving power at upper mantle depths.

THE EXPERIMENT

The field site is located within the Kapuskasing Structural Zone, lying within the Superior province of the central Canadian Shield (Fig. 1). The regional uniformity of the electrical structure of the mid- to lower crust, as well as the low conductance of the upper 15 km of the crustal section (~0.4 S) [Kurtz, et al, 1993] make this area a relatively homogeneous and resistive window through which the electrical structure of the upper mantle may be studied.

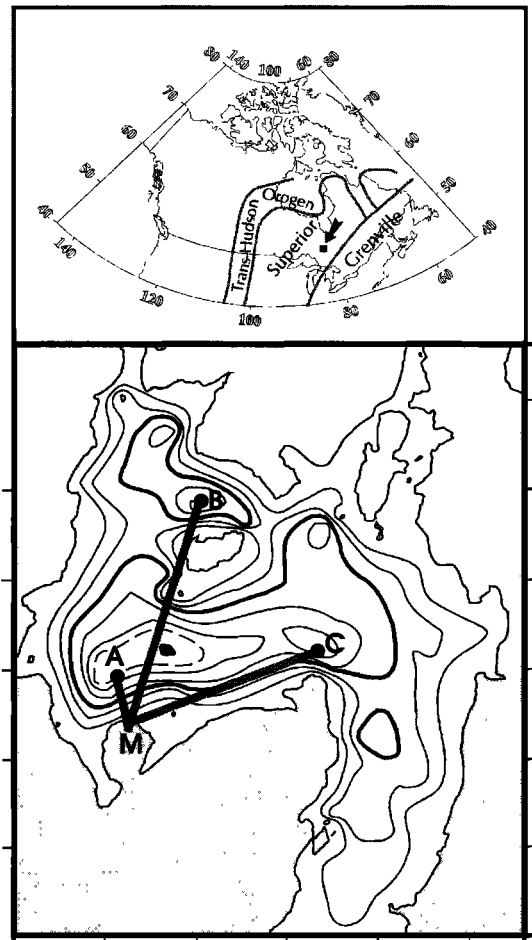


Figure 1. (Top) Location of field site. (Bottom) Orientation of electric field arrays and position of magnetometer (M). The electric receiver dipoles are (A-B) 1103.5 m long bearing  $27.8^\circ$  (true), (A-C) 1084.8 m long bearing  $84.3^\circ$ , and (B-C) 1034.8 m long bearing  $147.0^\circ$ , respectively. Lines running from shore are lakebottom cables. Contour intervals are 10 feet (3.05 m).

<sup>1</sup> Institute of Theoretical Geophysics, University of Cambridge

<sup>2</sup> Geological Survey of Canada, Ottawa

<sup>3</sup> Woods Hole Oceanographic Institution

Copyright 1993 by the American Geophysical Union.

Paper number 93GL02833

0094-8534/93/93GL-02833\$03.00

Three ~1 km long electric field dipole receivers were installed in June 1989 in 15 m of water in Carty Lake, Ontario [48°10'N, 82°42'W] (Fig. 1). The cables were each terminated with sets of two Ag-AgCl electrodes. Matched electrode pairs formed a triangular array, any two sides of which could be used to decompose the electric field into orthogonal components. Electric potential variations were recorded onshore in a buried insulated vault, with least count sensitivity of ~0.020  $\mu\text{V/m}$ , and 96 dB dynamic range. The magnetometer at this site, and a remote reference instrument 35 km SW, were triaxial ring core fluxgates with 0.025 nT least count sensitivity. At the lake site, magnetic fields were sampled at 8 Hz, electric fields at 1 Hz, and one minute median values were stored. Data recording ceased in March 1993.

The proximity of the field site to the auroral zone, and operation near the peak of the solar cycle, lead to frequent episodes of energetic, non-plane wave source field behaviour. Even with robust processing, response functions computed from these data were biased and non-causal. This problem was solved by implementing a modified form of Chave and Thomson's [1989] robust remote reference processing scheme which downweights both electric field outliers and magnetic field leverage points. Leverage point removal eliminated nearly 40% of the data. The resulting response tensor is well behaved at periods under ~10,000 s, but displays residual scatter at longer periods due to  $Sq$  bias. It also shows strong galvanic distortion, and the decomposition of Groom and Bailey [1989] with the addition of jackknife estimation of the response errors was applied. The resulting response is both causal and 1D at periods of 50 minutes to 3.5 days with weak 2D effects at shorter periods, hence the arithmetic mean of the off-diagonal response tensor terms was taken for further interpretation.

Extension of the MT band to 3.5 days and beyond overlaps in frequency with a GDS response from Cheltenham, Virginia, which is nearly free of galvanic distortion [Schultz & Larsen, 1987]. Although further from the lakebottom site than the nearest magnetic observatory at Ottawa (1145 km rather than 612 km), the complexity of the source field at Ottawa made calculation of a GDS response there difficult.

At higher frequencies, there is overlap between the lakebottom data, and MT data obtained from a previously occupied MT site 4 km S of Carty Lake [Kurtz, et al, 1993]. This was an element of an array of MT stations, making "horizontal spatial gradient sounding" (HSG) [Jones, 1980] possible, which is relatively free of static distortion. The off-diagonal terms of the MT response tensor from the site 4 km S were averaged after Groom-Bailey decomposition, and then shifted to match those calculated from HSG sounding in a band near 300 s. The lakebottom apparent resistivities were in turn shifted by a site gain of 0.5526 such that they matched the higher frequency, undistorted, values from the nearby site. The corrected result appears in Fig. 2.

Without static distortion removal, no 1D model exists that fits both the lakebottom MT data and the longer period GDS data. After distortion removal, 1D models may be constructed that jointly fit both lakebottom and long period GDS curves. This gives us considerable confidence that the static shift, fixed at both high and low frequency extremes, is correct. This situation is unique in that the very long period lakebottom MT data can be compared against undistorted responses free from static shift, at both high and low frequency ends. We therefore inverted the joint GDS and lakebottom MT response, estimated at a total of 33 frequencies.

#### MODELS

The  $D^+$  algorithm [Parker & Whaler, 1981] was used to test for the existence of a 1D inverse solution and to construct an extremal model consisting of infinitesimally thin layers of finite conductance (Fig. 3A and Table 1). The  $E(\chi^2)$  misfit was 66.0, whereas the  $D^+$  misfit was 55.6. There is no significant trend to the misfit vs. frequency. The response function is consistent with a 1D earth with no indication of systematic bias.

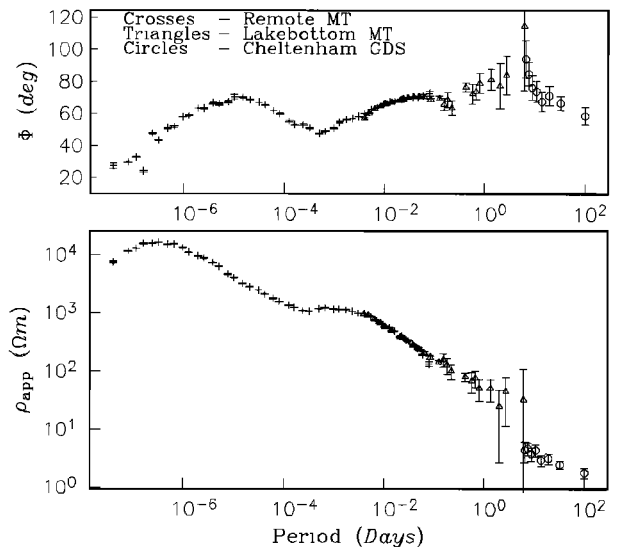


Figure 2.  $\rho_a$  and  $\phi$  with standard errors. MT curves are mean of undistorted off-diagonal impedance terms.

$D^+$  model space would have direct physical significance had we reason to believe that the upper mantle is extremely resistive, with local zones of enhanced conductivity rising above the underlying trend. Failing this,  $D^+$  assumes a more abstract role as a means of testing consistency with 1D, and as an objective providing the smallest possible  $\chi^2$  misfit to the data. It is notable, however, that the  $D^+$  conductor depths roughly coincide with the major seismic transitions from near-Moho, the ~205-230 km Lehmann discontinuity [Karato, 1992] (as well as the conductive layer often associated with the asthenosphere), the 410 km and 660 km velocity jumps [Bina, 1991], and ultimately terminating at depths beneath the core-mantle boundary. Any assertion that localised jumps in conductivity at these depths are strictly required by the data is premature, and will be tested below.

While  $D^+$  is the roughest possible model, the continuous model shown in Fig. 3A (thick curve) is the flattest. A regularised inversion [Smith & Booker, 1988] found the model fitting the data such that  $d(\log \sigma)/dz$  was minimised. All models that fit the data must have at least this degree of structure. To avoid the possibility of introducing unjustifiable structure into the inverse solution, we have fit to the ~98% confidence limit for a  $\chi^2_{66}$  variate, or 91, rather than to the  $E(\chi^2)$  misfit of 66. Given the careful attention paid to constructing meaningful error bars for the response functions, we are very unlikely to overfit the data at this level.

Above the overall upward trend below 100 km, zones of enhanced conductivity are found in the model, with peaks centred at depths of 280 km and 456 km, with a broader zone centred at 825 km. Resolving kernels centred at these depths appear in Fig. 3B. All three are symmetric and narrow, indicating the model conductivities

Table I:  $D^+$  Model Before and After Transformation to Spherical Earth Geometry

Cartesian	Cartesian	Spherical	Spherical
Depth(km)	Conductance(S)	$r_e$ - radius(km)	Conductance(S)
40	137	40	137
261	1833	261	1820
416	7425	417	7293
643	38387	647	36727
695	705650	701	669852
1790	2007568	1915	1292758
2750	$\infty$	3459	$\infty$

here represent local averages. This conservative view of the conductivity structure persists in requiring inflexions in  $\log \sigma$  at depths near the major mantle seismic transitions.

We deleted the 13 response values at periods found uniquely in the lakebottom MT data,  $2 \text{ hours} \leq T \leq 6 \text{ days}$ , and inverted the remaining 20 values corresponding to the higher frequency data available from the previously occupied nearby MT site and from the lower frequency GDS responses. The thin curve in Fig. 3A is the flattest model that fits the depleted data with the same relative misfit as before. Peaks in  $\log \sigma$  are found near 280 km and 809 km and have similar resolving kernels to the corresponding peaks in the model from the complete dataset. The previously well resolved conductor near 456 km is absent from this model, and its conductance is smeared over greater depths. The addition of lakebottom MT data at  $2 \text{ hours} \leq T \leq 6 \text{ days}$  makes it possible to resolve the conductivity jump at these depths.

The  $H^+$  nonlinear inversion [Parker & Whaler, 1981] finds models consisting of a number of slabs, each of which must have the same layer parameter ( $d^2 = \sigma h^2$ ;  $h$  is layer thickness). Only  $H^+$  models (not shown here) with  $d^2 \leq 113 \text{ s}$  fit the data. In contrast,  $H^+$  models from lower resolution GDS data typically consist of one or two conductive slabs with  $10^4 \leq d^2 \leq 10^8 \text{ s}$ . In the present case, fine scale structure in the response functions arises from fine scale structure in the lower crust or upper mantle (hence small  $d^2$ ). As a result,  $H^+$  fails to fit the joint MT/GDS data other than with  $D^+$ -like models, i.e. abrupt and localised jumps in conductivity at depths nearly coincident with the seismic transitions.

While the existence of rapid jumps in  $\log \sigma$  is indicated, the inversions thus far have not established the maximum thickness of these zones. A corollary is whether the dips in conductivity beneath the peaks are strictly required by the data. The use of the linearised minimum structure inversion would suggest that they are, but a fully nonlinear approach, free from the  $H^+$  restriction of finding only best fitting constant  $d^2$  models is necessary to confirm this.

We have implemented a nonlinear inversion and hypothesis testing approach using a genetic algorithm (GA). For the 1D MT case, it is possible to show (paper in preparation) that the GA asymptotically converges to the global minimum, or  $D^+$  solution. This is a powerful property since by placing a priori bounds on the range of acceptable  $\log \sigma$  for any given layer, we can test whether any model exists that fits the data given those bounds.

We have overparameterised the earth into as many as 41 fixed thickness layers, spanning 0 to 1300 km depth, terminating in a half-space. The GA locates acceptable models ( $\chi^2 \leq 91$ ) given prior bounds of  $-5 \leq \log \sigma \leq 1.4 \text{ S/m}$ . Conversely, no acceptable models are found if  $\log \sigma$  is not permitted to rise above -2.4 between depths of 225-325 km, or above -2.0 between 400-550 km (the approximate baselines above which the conductive peaks rise in the flattest model).

We have also made layer thickness a free parameter, and have been unable to construct any 5 or 6 layered variable thickness models ( $2 \leq h \leq 200 \text{ km}$  and  $-5 \leq \log \sigma \leq 0.3 \text{ S/m}$ ) that fit the data without abrupt increases in  $\log \sigma$  near 230, 425, and 660 km. Five layer variable thickness models can be found without a dip beneath the 261-280 km peak. A dip below the 416-456 km peak is always an element of the models, unless we impose a positivity constraint on the inversion ( $d(\log \sigma)/dz > 0$ ;  $z > 220 \text{ km}$ ). In this case, the best fitting 5 layer model with monotonically increasing  $\log \sigma$  ( $z > 220 \text{ km}$ ) has a misfit of  $\chi^2 = 90$ . This answers the question posed earlier, i.e. it is possible to (nearly) fit the data by a model with monotonically increasing conductivity below 220 km depth. No 4 layer model can be found that fits the data within the same tolerance. Such underparameterised models do not permit a dip in  $\log \sigma$  beneath 416-456 km. The persistence of this feature suggests that the elevated conductance at these depths may be concentrated within a thin zone.

A range of preferred models, compended from the flattest linearised inversion as well as fixed and variable thickness GA model searches, is seen in Fig. 4. The flattest model and the GA models with thickest layers (conservatively (under)fit to the 98% confi-

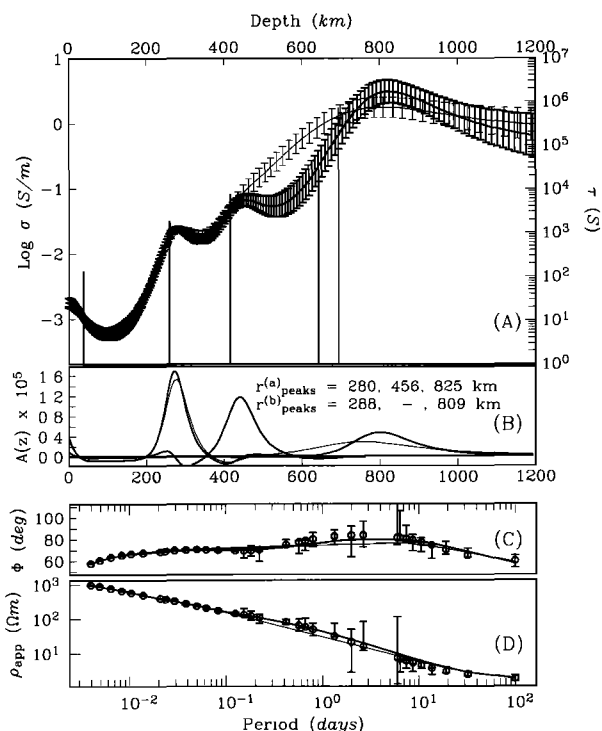


Figure 3. (A) Flattest conductivity model with confidence limits for full (thick) and depleted (thin) datasets; and  $D^+$  model (vertical bars). Left-hand axis gives conductivity scale, right-hand axis  $D^+$  conductance scale. (B) Resolving kernels for depths centred on conductive zones in flattest models. (C) Fit of flattest model for full (thick) and depleted (thin) datasets, and of  $D^+$  (symbols) model to MT response plotted as standard errors on phase. (D) as (C) but apparent resistivity. Longest 8 periods are GDS response, remaining 25 periods are undistorted lakebottom MT response.

dence limit) all have very  $D^+$ -like thin, abrupt, conductive jumps. The conductivity within narrow zones beneath these jumps is quite restricted.

## DISCUSSION

We have detected rapid increases in upper mantle conductivity within three discrete zones. It is, however, impossible to exclude models containing highly resistive regions between the more conducting layers. Only the conductance (integrated conductivity) of the mantle is independently constrained by MT and GDS data.

A lower bound on the conductance of the region between 660 km depth and the core-mantle boundary (see Table 1) is  $2.713 \times 10^6 \text{ S}$ , or an average of  $\sigma = 1.32 \text{ S/m}$  for this zone. This is incompatible with the upper bound of  $10^{-3} \text{ S/m}$  reported by Li and Jeanloz [1987] from diamond anvil measurements of silicate perovskite and of perovskite-magnesiowüstite under lower mantle P-T conditions. Conversely, our results are in reasonable agreement with laboratory work by Peyronneau and Poirer [1989] on San Carlos xenoliths.

Predicted values for  $\sigma$  at 250-660 km depth have been generated using Akaogi et al's [1989] geotherm, and an empirical relation between  $\sigma$  and  $T$  for dry olivine [Shankland and Duba, 1990] (Fig. 4). A pyrolytic bulk composition above 660 km is assumed, with olivine composition of  $(Mg_{0.89}, Fe_{0.11})_2SiO_4$  and an adiabatic temperature gradient below 390 km. With the exception of the zone of enhanced  $\sigma$  near 261-280 km, the predicted conductivities lie within the poorly defined resistive bounds of the preferred model. Interpolating between the predicted values would, however, lead to

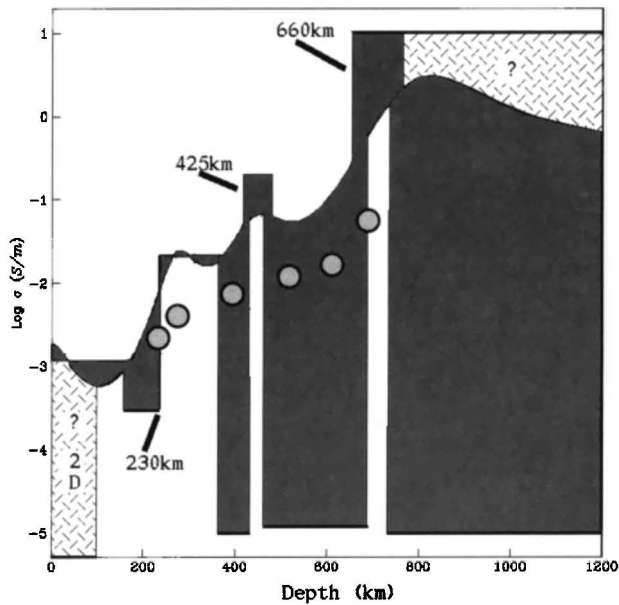


Figure 4. Range of preferred models. Dark shaded area is bounded by variable layer thickness GA models, and by flattest continuous model. The shallow lightly shaded region are depths at which the response is weakly 2D. The deeper lightly shaded region is poorly constrained according to the fixed layer thickness GA. The large dots are log conductivities calculated from a petrologic model.

an upper mantle with total conductance nearly an order of magnitude lower than that supported by the field data. If the laboratory measurements are representative of in situ equilibrated conditions, then either the upper mantle geotherm is erroneously biased downward, or the use of a simple dry olivine model is incorrect. Furthermore, the direct transformation of any given inverse conductivity model into an equivalent geotherm is a delicate matter. The flattest model is intuitively appealing, yet it remains only one of an infinity of acceptable models whose bounds are shown in Fig. 4.

At 1300°C and 50-300 MPa, olivine can accommodate as much as 0.0034 wt % water [Bai and Kohlstedt, 1992]. Water concentration in the upper mantle may be 0.001-0.1 wt %, thus olivine grains may be the dominant water storage location in the mantle, and  $\sigma$  may be elevated substantially above the dry phase assumed above.

Our results may be contrasted with Egbert and Booker [1992] who inverted joint MT/GDS responses from historical data from Tucson. Their responses systematically deviate from 1D form for periods of ~1-4 days and shorter, possibly due to proximity to the upwelling asthenosphere associated with the active tectonism of the SW US. They carried out 1D inversion of this non-1D response, and report approximately an order of magnitude higher conductance in the upper 200 km of the mantle than we find, with shallower slope, leveling to ~1 S/m at 1000 km. The jump in  $\sigma$  we identify near 416-456 km is absent from their models. The Canadian Shield data are consistent with 1D interpretation at depths below about 100 km.

It is natural to associate the conductivity jump near 416-456 km with the olivine-spinel transition. This observation was anticipated by Akimoto and Fujisawa [1965] who noted variations in  $\sigma$  over this phase transition, a result disputed by recent shock measurements. There is evidence from our work that upper mantle conductivity may not increase monotonically with depth. The 416-456 km peak may be underlain by more resistive material. This is the first MT result of sufficient resolution to identify and require a discrete conductivity jump around this depth range, and suggests much work remains to be done in examining the sensitivity of conductivity to the olivine-spinel transition, and any mechanisms for non-monotonic dependence of conductivity with depth.

**Acknowledgments.** This research was supported by National Science Foundation Grants EAR87-21223 and EAR91-21278. We thank R. Groulx, J. Craven, E. Berndt & R. Groom for their field assistance. Contribution number 3359, Department of Earth Sciences, University of Cambridge. WHOI contribution number 8442. Geological Survey of Canada Contribution 20593. Lithoprobe Publication 478.

#### REFERENCES

- Akimoto, S., and H. Fujisawa, Demonstration of the electrical conductivity jump produced by the olivine-spinel transition, *J. Geophys. Res.*, 70, 443-449, 1965.
- Akiogi, A., E. Ito, and A. Navrotsky, Olivine modified spinel-spinel transitions in the system  $Mg_2SiO_4-Fe_2SiO_4$ : Calorimetric measurements, thermomechanical calculation, and geophysical application, *J. Geophys. Res.*, 94, No. B11, 15,671-15,685, 1989.
- Bai, Q. and L. Kohlstedt, Substantial hydrogen solubility in olivine and implications for water storage in the mantle, *Nature*, 357, 672-674, 1992.
- Bina, C.R., Mantle discontinuities, *Rev. Geophys. Suppl.*, 783-793, 1991.
- Chave, A.D., and D. J. Thomson, Some comments on magnetotelluric response function estimation, *J. Geophys. Res.*, 94, No. B10, 14,215-14,202, 1989.
- Egbert, G.D., and J.R. Booker, Very long period magnetotellurics at Tucson observatory: Implications for mantle conductivity, *J. Geophys. Res.*, 97, No. B11, 15,099-15,112, 1992.
- Groom, R.W., and R.C. Bailey, Decomposition of magnetotelluric impedance tensors in the presence of local three-dimensional galvanic distortion, *J. Geophys. Res.*, 94, No. B2, 1913-1925, 1989.
- Jones, A. G., Geomagnetic induction studies in Scandinavia - I. Determination of the inductive response function from the magnetometer data, *J. Geophys.*, 48, 181-194, 1980.
- Karato, S., On the Lehmann discontinuity, *Geophys. Res. Lett.*, 19, No. 22, 255-2258, 1992.
- Kurtz, R.D., et al, The conductivity of the crust and mantle beneath the Kapuskasing Uplift: Electrical anisotropy in the upper mantle, *Geophys. J. Int.*, 113, 483-498, 1993.
- Li, X. and R. Jeanloz, Electrical conductivity of (Mg,Fe)SiO<sub>3</sub> perovskite and a perovskite-dominated assemblage at lower mantle conditions, *Geophys. Res. Lett.*, 14, 1075-1078, 1987.
- Parker, R.L., and K.A. Whaler, Numerical methods for establishing solutions to the inverse problem of electromagnetic induction, *J. Geophys. Res.*, 86, 9574-9584, 1981.
- Peyronneau, J., and J. P. Poirer, Electrical conductivity of the Earth's lower mantle, *Nature*, 342, No. 6249, 537-539, 1989.
- Schultz, A., and J. C. Larsen, On the electrical conductivity of the mid-mantle: 1- Calculation of equivalent scalar magnetotelluric response functions, *Geophys. J. R. astr. Soc.*, 88, 733-762, 1987.
- Schultz, A., J.R. Booker and J.C. Larsen, Lakebottom magnetotellurics, *J. Geophys. Res.*, 92, 10639-10649, 1987.
- Shankland, T.J., and A.G. Duba, Standard electrical conductivity of isotropic olivine in the temperature range 1200-1500°C, *Geophys. J. Int.*, 103, 25-32, 1990.
- Smith, J.T., and J.R. Booker, Magnetotelluric inversion for minimum structure, *Geophysics*, 53, No. 12, 1565-1576, 1988.

A. Schultz, Institute of Theoretical Geophysics, Department of Earth Sciences, Downing Street, Cambridge CB2 3EQ, England.

A. Chave, Woods Hole Oceanographic Institution, Woods Hole, Massachusetts, 02543, USA.

A. Jones and R. Kurtz, Geological Survey of Canada, 1 Observatory Crescent, Ottawa, Ontario K1A 0Y3, Canada.

(Received 18 June, 1993;  
revised 7 September, 1993;  
accepted 21 September, 1993)